Bulging Distortion of Austenitic Stainless Steel Sheet on the Partially Penetrated Side of Non-Penetration Lap Laser Welding Joint

Chengwu Yao (yaochwu@sjtu.edu.cn)
Shanghai Jiao Tong University https://orcid.org/0000-0002-3407-8717
Enze Liu
Shanghai Jiao Tong University
Jiaming Ni
Shanghai Aerospace Precision Machinery Institute
Binying Nie
Yichun University

Original Article

Keywords: non-penetration lap laser welding, bulging distortion, austenitic stainless steel, compressive stress, tension stress.

Posted Date: May 6th, 2021

DOI: https://doi.org/10.21203/rs.3.rs-469058/v1

Version of Record: A version of this preprint was published at Chinese Journal of Mechanical Engineering on January 16th, 2024. See the published version at https://doi.org/10.1186/s10033-023-00987-2.

Abstract

Non-penetration laser welding of lap joints in austenitic stainless steel sheets is commonly preferred in fields where the surface quality is of utmost importance. However, the application of non-penetration welded austenitic stainless steel parts is limited owing to the micro bulging distortion that occurs on the back surface of the partial penetration side. In this study, non-penetration lap laser welding experiments, were conducted on galvanized and SUS304 austenitic stainless steel plates using a fiber laser, to investigate the mechanism of bulging distortion. A comparative experiment of DC01 galvanized steel-Q235 carbon steel lap laser welding was carried out, and the deflection and distortion profile of partially penetrated side of the sheets were measured using a non-contact laser interferometer. In addition, the cold-rolled SUS304 was subjected to heat holding at different temperatures and water quenching after bending to characterize its microstructure under tensile and compressive stress. The results show that, during the heating stage of the thermal cycle of laser lap welding, the partial penetration side of the SUS304 steel sheet generates compressive stress, which extrudes the material in the heat-affected zone to the outside of the back of the SUS304 steel sheet, thereby forming a bulge. The findings of these experiments can be of great value for controlling the distortion of the partial penetrated side of austenitic stainless steel sheet during laser non-penetration lap welding.

1. Introduction

Austenitic stainless steel and galvanized steel sheet joints are commonly used in decorative structures, household kitchen utensils, buildings, elevators, and architectural trim panels. Furthermore, they have the advantages of better appearance, corrosion resistance and cost effectiveness. In these application areas, even though the strength requirements for thin-plate joints are low, good appearance is extremely strict; and any defect on the surface of the austenitic stainless steel sheet, can reduce the consumer's subjective evaluation of the product. Gluing and various welding methods like non-penetration welding are commonly used for joining such sheets. Glued joints have various advantages over welding such as no distortion, and lower processing difficulty, but the disadvantages of glued joints are also serious. The glued joints are deteriorated with time, and joint failure can easily occur [1]. In contrast, the mechanical properties of non-penetration welded joints remain stable, and the surface integrity of the partially penetrated side of the austenitic stainless steel can be guaranteed [2, 3]. The energy of Laser welding is more concentrated than other welding methods, and its welding heat affected zone is smaller as well [4]. Therefore, non-penetration laser lap welding may be an alternative to gluing for such stainless steel sheet lap joints with higher surface quality requirements[5–7]. However, in this type of welding, micro bulging distortion occurs on the non-penetration side of the austenitic stainless steel plate. Even though this distortion is of micron scale, it seriously affects the surface quality of the welded joint. This is a serious problem and needs to be solved urgently.

Many researchers have done studies on various types of distortion s occurring during the laser welding process of thin plates. H. Huang et al. [8] studied the welding deformation of thin plates based on the

inherent strain theory, and considered that the deformation of butt welding of thin plate is generally produced by the longitudinal and transverse inherent strains. S. Matsuokaa [9] studied the thermal distortion of thin stainless steel sheet in the bead-on-plate welding by using a single mode fiber laser with a Galvano scanning system, and concluded that the angle deformation of thin stainless steel sheet in laser micro-welding was due to both the shrinkage of width direction related to humping and the expansion of weld bead with the convex curvature on the top surface. M Choobi [10] considered the laser welding deformation of thin plates is mainly angular deformation, and used a self-built artificial neural network model to reproduce the angular deformation that occurred during the welding of SUS304 stainless steel sheets. Liu Jia [11] studied the non-penetration lap laser welding of SUS301 stainless steel plates of thickness 0.8 mm and 1.2 mm, and concluded that the deformation of SUS301 stainless steel plate on the partially penetrated side is an angular deformation mechanism. So far, the researches on laser welding distortion of thin plates mainly focused on large-scale macroscopic deformations, such as angular deformation, and very few studies focused on micron scale deformation of thin plate. The engineers of some elevator panel manufacturing companies used the method of correcting the angular deformation to eliminate the bulging distortion of the partially penetrated side of austenitic stainless steel sheet, but it had almost no effect, so non-penetration lap laser welding method has not used in the manufacture of elevator panels.

In this paper, the influence of laser power on the bulging distortion degree of the partially penetrated side of the lap welded joint of DC01 galvanized steel and SUS304 stainless steel sheet was studied, and it was compared with the lap joint of DC01 galvanized steel and Q235 carbon steel sheet.. In addition, by characterizing the microstructure of the cold-rolled SUS304 stainless steel sheet after heat holding at 300℃-1000℃, bending and water quenching, and comparing it with the microstructure of the bulging distortion zone of the SUS304 stainless steel sheet, the welding thermal cycle peak temperature and stress type of the bulging distortion zone in the partially penetrated side of SUS304 stainless steel sheet were obtained. Based on the above experiments, the distortion mechanism of the bulging distortion which occurred on the partially penetrated side of the SUS304 austenitic stainless steel sheet was discussed. These results can be very valuable for successful applications of non-penetration laser lap welding to austenitic stainless steel sheet components with high appearance quality requirements.

2. Materials And Methods

DC01 galvanized steel sheet and SUS304 austenitic stainless steel sheet each of size 110×110 mm, were used in the non-penetration lap laser welding experiments. The thickness of both DC01 galvanized and the SUS304 stainless steel sheets are 1.2 mm, and the SUS304 stainless steel sheet is the lower plate of the lap joint, which is in a cold-rolled state. The cold-rolled Q235 carbon steel sheet of the same size was also used, for the non-penetration lap laser welding joint of DC01 galvanized steel-Q235 carbon steel sheet. The chemical compositions of the test steel sheets used, are shown in Table 1, therein the thickness of the zinc layer of DC01 steel is 2.5um.

Table 1
Chemical compositions of SUS304 austenitic stainless steel, DC01 galvanized steel, and Q235 steel

Plates	Elements/wt.%								
	C	Mn	P	S	Si	Cr	Ni	Al	Fe
SUS304	0.027	1.6	0.01	0.002	0.36	18.5	11.6	/	Bal
DC01	0.1	0.5	0.035	0.025	/	/	/	0.02	Bal
Q235	0.14	0.55	0.025	0.008	0.19	/	/	/	Bal

The YLS-10000 fiber laser produced by American IPG Company was used in the experiment. Zero defocus welding was adapted with the Gaussian beam diameter at the focus being 0.72 mm and the wavelength of λ = 1070–1080 nm. The welding speed is controlled by Japanese FANUC robot. Pure laser welding was used for lap welding. The laser power is 1.9–2.6 kW, and the welding speed is 70 mm/s.

Figure 1a is a schematic of non-penetration laser welding system. Figure 1b is the photo of the welding fixture. The two sheets to be welded are stacked in a jig groove, the upper one is the DC01 galvanized steel sheet, and the lower one is the SUS304 stainless steel sheet. Two pressure plates are respectively pressed on the two sides of the test sheets to be welded, and the bolts are screwed onto the pressure plate through bolt holes. The digital display detection torque wrench is used to tighten the bolts. In order to ensure that the clamp force of the sheet stack for each welding experiment is the same, the tightening torque of each bolt is set to 5500N.m. During laser welding, the laser illuminates the surface of the sheets in the middle groove region of the clamp, and the penetration depth of the SUS304 stainless steel sheet is controlled by adjusting the laser welding process parameters, to form a partially penetrated welded joint.

Due to the too small size of the bulging formation zone on the back surface of partially penetrated side of SUS304 stainless steel sheet, it is difficult to accurately measure the peak temperature of this zone during lap laser welding. Therefore, an experimental simulation method was used to obtain the peak temperature of the welding thermal cycle of the bulging formation zone. The cold-rolled SUS304 stainless steel was heated to 300 ℃, 400 ℃, 500 ℃, 600 ℃, 700 ℃, 800 ℃, 900 ℃, 1000 ℃, respectively, and quenched immediately after 5 minutes of heat preservation. The microstructure of SUS304 stainless steel sheets after heating at different heat treatment temperatures was characterized. By comparing it with that the microstructure of the bulging distortion zone of partially penetrated side of SUS304 non-penetration welded joint, the peak temperature of the welding thermal cycle of the bulging distortion zone during lap laser welding was obtained. The cold-rolled SUS304 stainless steel sheet was heated at this peak temperature, bent and quenched, and the microstructure of the bent sheets under compressive stress of the interior arc and the tensile stress of the exterior arc were obtained. By comparing it with the microstructure of lap laser welded joint, the type of stress generated in bulging distortion zone was obtained.

The cross-sections of non-penetration lap welding joints of DC01 galvanized steel-SUS304 stainless steel, and DC01 galvanized steel-Q235 carbon steel, along with SUS304 stainless steel heat treated samples, were etched by aqua regia after grinding and polishing. The microstructures of the welded joints were observed by MCK-50MC metallographic microscope produced by Zeiss, and an electron scanning microscope of NOVA NanoSEM 230 produced by FEI. The ZeGage 3D surface profiler manufactured by ZYGO Co., Ltd., was used to measure the micro bulging distortion on the surface of the non-melting side of the austenitic steel sheet. The profiler shoots a specific wavelength of laser light onto the surface of the sheets to be tested. Then, it receives the reflected light from the surface of the sheet, and processes it in a computer to obtain surface topography data of the material to be tested.

3. Results And Discussion

Figure 2 shows the macro morphologies of non-penetration lap welded joints of DC01-sus304 and DC01-Q235 steel sheets, with welding speed of 70 mm/s and laser power of 2.0 kW. The weld is well formed without any obvious macro defects. It must be pointed out that, even if the penetration depth of the lap weld is only about 0.1 mm, a steep peak is still formed on the back of the partially penetrated side of lap welded joints of DC01-SUS304 steel sheets, with a peak height of about 6μm, as shown by the red arrow in Fig. 2a. On the contrary, the bulging distortion of partially penetrated side of lap welded joints of DC01-Q235 steel sheets is gentle, as shown by the arrow in Fig. 2b, and there is a flat peak on the partially penetrated side, with a peak height of about 3μm.

3D model of the bulging profile on the partially penetrated side of lap welded joint of DC01 galvanized steel-SUS304 steel sheets, as obtained by the profilometer is shown in Fig. 3, in which different colors represent the relative height of different positions. Figure 3a shows a bulging profile model with the profilometer scanning width of 8 mm and laser power of 2.4 kW. It can be seen from Fig. 4a that the distortion exhibits obvious angular deformation, but the bulging profile is mainly in the range of 2 mm in width. From the visual inspection of decorative parts, visual distortion will reduce the subjective evaluation of the surface quality of the material. Generally, steep peaks will cause large height fluctuations on the surface of the parts, which will change the reflection path of the incident light and cause visual distortion. Therefore, the visually distorted area on the partially penetrated side of the SUS304 steel sheet should also be the bulging distortion zone within a width of 2 mm. In view of this, the following research focuses on this 2mm bulging distortion zone. Figure 3b, Fig. 3c, and Fig. 3d show the bulging profile models on the partially penetrated side of lap welded joints with a welding speed of 70mm/s, and a laser power of 0 kW, 2.0 kW, and 2.6 kW, respectively. In the range of 2mm in width, the maximum peak heights are 0μm, 6μm, and 27μm, respectively.

In order to describe the bulging distortion more directly, the position data of the 3D model of the bulging profile was derived from the profilometer, and the 2D profile of the bulging distortion in the vertical welding direction was drawn based on these data, as shown in Fig. 4. The profile of the bulging distortion zone of the lap welded joint of galvanized steel-SUS304 stainless steel sheets is shown in Fig. 4a. The region with the most obvious distortion, between two dotted lines, is at the center of the weld, and its

width is about 2 mm. The profile of the bulging distortion is substantially a bilaterally symmetrical curve. When the laser power is lower than 2.0 kW, the curve is gentle, and the radius of curvature at the peak is large, and the slope of each point in the curve remains stable, indicating that the bulging distortion has the characteristic of angular distortion. As the laser power increases, the curve becomes steeper, the radius of curvature at the peak gradually decrease. When the laser power is increased to 2.2 kW or higher, the slope of the curve increases sharply, and the angular deformation feature of the bulging distortion zone disappears. Figure 4b shows the outline curve of the bulging distortion zone of the lap welded joint of galvanized steel-Q235 steel sheets. When the laser power is 2.0 to 2.8 kW, the partially penetrated side of Q235 steel sheet, does not show the sharp bulging distortion similar to that of SUS304 stainless steel sheet, but shows the feature of angular deformation.

By comparing Fig. 4a and Fig. 4b, it is found that the peak of the curve of the bulging distortion zone of Q235 steel sheet is lower than that of SUS304 steel sheet, and the slope of the curve is also lower than that of SUS304 steel sheet. For example, the lap laser power is 2.6 kW, the peak height of the contour curve of the bulging distortion zone of Q235 steel sheet is about 5μm, and the slope is about 0.005, while the peak height of the curve of SUS304 steel sheet is about 27μm, and the slope is about 0.024. Since the slope of the curve of the deformation zone of the Q235 carbon steel sheet is small, it has less influence on the reflected light, which will not cause visual distortion and deteriorate the surface quality of Q235 steel sheet.

Figure 5 shows the macroscopic morphology and microstructure of the SUS304 sheet on the partially penetrated side of the lap welded joint of DC01 galvanized steel-SUS304 stainless steel sheets. Figure 5a shows the morphology of the partially penetrated side of the lap welded joint. The welding heat-affected zone of the SUS304 steel sheet is in the shape of "V". Figure 5b shows the overheated zone near the fusion line, where the elongated original grains in the cold-rolled state, are completely recrystallized into coarse equiaxed grains. As shown in Fig. 5c, in the heat affected zone far from the fusion line, the recrystallized equiaxed grains become finer. Figure 5d shows, that even in the edge of the SUS304 stainless steel sheet, the original cold-rolled grains still disappear, and the elongated grains almost completely recrystallized into equiaxed grains. Figure 5e shows the EBSD image of the bulging distortion zone of the back surface of the SUS304 steel sheet, as shown by the arrow, there are a large number of sub-grains in the equiaxed grains, indicating that stress plastic distortion is accompanied by the formation of equiaxed grains.

Twins were observed in these equiaxed grains in the heat-affected zone of the SUS304 steel sheet, and the twins generated at different positions have different morphologies. As shown in Fig. 5b and Fig. 5c, these regions have higher temperatures due to being closer to the fusion line, resulting in coarser recrystallized equiaxed grains, and twins are also coarse and traverse the entire grains, which are typical annealing twins. The bulging distortion zone is located at the edge of SUS304 steel sheet, which has fine recrystallized equiaxed grains because it is far from the fusion line, as shown in Fig. 5d. A large number of densely-concentrated clusters of fine twins appear in the equiaxed grains, as shown by the red arrows, and the twin planes of these twins tend to be perpendicular to the cold rolling direction of the SUS304

steel sheet. These twins are lenticular, originate from the grain boundaries and end in the interior of the grains, which are typical deformation twins. Figure 6 shows the water-quenched microstructure of the cold-rolled SUS304 steel sheet held at 300°C to 700°C for 5 minutes. After being held at 300°C to 700°C for 5 minutes, the cold-rolled SUS304 sheet was in the recovery stage, and its grain morphology was still in the form of fibers elongated in the rolling direction, as shown in Fig. 6a to Fig. 6e. After being held at 850°C for 5 minutes, a small amount of annealed twins appeared in the cold-rolled SUS304 sheet, as shown in Fig. 6f. After being held at 900°C for 5 minutes, a small amount of recrystallized equiaxed grains appeared, as shown in Fig. 6g. After being held at 1000°C for 5 minutes, as shown in Fig. 6h, a large number of the recrystallized equiaxed grains and annealing twins appeared in the cold-rolled SUS304 steel sheet, which was similar to the microstructure of the welding heat-affected zone of the SUS304 steel sheet, as shown in Fig. 5. Therefore, the effect of heat treat at 1000°C *5 minutes on the microstructure of the cold-rolled SUS304 steel sheet was similar to that of the peak temperature of the thermal cycle of lap laser welding on the microstructure of the bulging distortion zone.

In order to analyze the type of stress that caused the deformation twins to be generated in the bulging distortion zone of the non-penetration lap welded joint, the cold-rolled SUS304 steel sheet was held at 1000°C for 5 minutes, and then immediately bent and quenched. Figure 7a shows the macroscopic shape of the bent cold-rolled SUS304 steel sheet. According to the stress distribution theory of plane bending structure, the outer arc of the bent SUS304 sheet is subjected to tensile stress σ_T, and the inner arc is subjected to compressive stress σ_C. Figure 7b shows the optical micrograph of the inner arc of the bent SUS304 sheet, where the recrystallized equiaxed grains are compressive into flat grains by compressive stress. Due to the preferential twins caused by compressive stress, the twin plane of annealed twins tends to be perpendicular to the compressive stress, that is, perpendicular to the rolling direction of the cold-rolled SUS304 sheet, as shown by the light blue arrows. In addition, the dense deformation twins occur in the inner arc of the bent sheet, as shown in Fig. 7c, and their direction is also perpendicular to the rolling direction of the cold-rolled SUS304 sheet. The recrystallized grains in the outer arc of the bent SUS304 sheet are elongated by tensile stress, as shown in Fig. 7d. The twin plane of annealed twins tends to be parallel to the tensile stress, that is, parallel to the rolling direction of the cold-rolled SUS304 sheet, as shown in Fig. 7e. Due to the absence of stress, the recrystallized equiaxed grains in the center of the bent SUS304 sheet still retain the polygonal shape, and the twin planes of the annealed twins have no obvious directionality, as shown by the yellow arrow in the Fig. 7f.

Comparing Fig. 5 and Fig. 7, the deformation twins formed in the bulging distortion zone of the SUS304 steel sheet of the lap welded joint are similar to the deformation twins formed in the inner arc of the bent SUS304 sheet. Therefore, it can be inferred that the type of stress that caused the bulging distortion of the partially penetrated side of SUS304 steel sheet is the same as the type of the stress in the inner arc of the bent SUS304 sheet, that is, compressive stress. However, non-penetration lap laser welding of thin plates did not always lead to steep bulging distortion. As shown in Fig. 4b, the curve of the distortion zone of the lap welded joint of the DC01 galvanized steel-Q235 carbon steel sheet was a flat slope, which may be due to the lower compressive stress on the partially penetrated side of the Q235 steel sheet.

In this research, the SUS304 and Q235 sheets are clamped by the rigid support of the clamp, with an opening for laser welding, as shown in Fig. 1, there is rigid restraint in the width direction of the non-penetration lap welded joints. During the laser welding process, the heat-affected zone (the "V" shaped area shown in Fig. 5a) on the partially penetrated side thermally expands, and due to the constraint from the lower temperature materials on both sides of this zone, compressive stress is generated. The thermal expansion coefficient of SUS304 stainless steel is $18.4\times10^{-6}/℃$, which is about 167% of that of Q235 steel ($11\times10^{-6}/℃$) at the same temperature. The thermal conductivity of SUS304 stainless steel is 12 $W.m^{-1}*K^{-1}$, which is only about 23% of that of Q235 steel (51 $W.m^{-1}*K^{-1}$) [12, 13]. Therefore, the thermal expansion of the SUS304 sheet in the heat-affected zone is much higher than that of Q235 carbon steel, which causes the compressive stress generated on the partially penetrated side of the SUS304 sheet to be greater than that of the Q235 sheet. Due to the small thickness of the sheet, the heat-affected zone can easily extend to the back side of the partially penetrated side of lap welded joint. Comparing Fig. 5d and Fig. 6g, the instantaneous temperature of the welding thermal cycle in the bulging distortion zone of the SUS304 sheet is above 900°C, which causes the tensile strength of the SUS304 sheet to drop sharply below 90 MPa. Therefore, even if the compressive stress is low, the material in the heat-affected zone of SUS304 sheet will be plastically deformed.

According to the above analysis, the deformation mechanism of the bulging distortion on the non-penetration side of austenitic stainless steel sheet, can be described as follows: as shown in Fig. 8a, the expansion of the "V"-shaped heat-affected zone on the partially penetrated side of the SUS304 sheet, is constrained by the adjacent low temperature zone and the rigid of the clamp on the overlapped steel sheets, and generates compressive stress. Consequently, the metal in the heat-affected zone ("V" shaped HAZ) is “extruded” by the compressive stress. Due to the high welding thermal cycle temperature, the strength of the SUS304 austenitic stainless steel sheet on the partially penetrated side of the lap welded joint is lower than the compressive stress, which causes the metal in the heat-affected zone of the SUS304 sheet to be extruded out of the back plane, thereby forming the bulging distortion. Since the extrusion deformation is formed in the tiny area of the heat-affected zone on the back of the SUS304 sheet, the peak of the bulging distortion forms is steep. As the temperature decreases, the weld pool solidifies and shrinks gradually, which causes the transition from the compressive stress to the tensile stress in the "V" shaped HAZ, as shown in Fig. 8b. After the lap welded joint is cooled to room temperature and the clamps are released, the tensile stress causes the angular deformation of SUS304 stainless steel sheet, as shown in Fig. 8c, while the bulging distortion is still retained.

4. Conclusions

According to the research in this paper, the Q235 carbon steel sheet on partially penetrated side of laser lap welded joint only shows angular deformation, while the SUS304 austenitic stainless steel sheet shows steep bulging distortion. SUS304 austenitic steel has higher thermal expansion coefficient and lower thermal conductivity than Q235 carbon steel, so higher compressive stress is generated on the partially penetrated side of the SUS304 steel sheet of the the lap welded joint, which causes the metal in

the heat-affected zone to be extruded out of the back plane of the SUS304 sheet, thereby forming the bulging distortion. The bulging distortion of the SUS304 sheet is formed in the heating stage of the laser welding thermal cycle, which is different from the angular deformation of the Q235 plate formed in the cooling stage of the welding thermal cycle. Therefore, in the practical engineering application of non-penetration lap laser welding, it is difficult to reduce the bulging distortion of the partially penetrated side of the austenitic stainless steel sheet to improve its surface quality by adopting measures to control angular deformation. Since the bulging distortion is formed in the tiny area of the heat-affected zone of austenitic stainless steel sheet, the effective measures may be to cut the peak of the compressive stress in the heat-affected zone by applying tensile stress.

Declarations

Availability of data and materials

All data generated or analyzed during this study are included in this published article.

Competing interests

The authors declare that they have no competing interest.

Contributions

Chengwu Yao conceived ideas, methodology, performed microstructural; Enze Liu conducted experiments, prepared the analysis of microstructure, prepared manuscript; Jiaming Ni carried out one part of microstructural analysis; Binying Nie revised the manuscript. All authors read and approved the final manuscript.

Acknowledgements

The authors sincerely thank Hitachi (China) Research & Development Corporation for their help with the welding process.

Funding

Not applicable.

References

1. MA Hai-Quan, Wang Qian-ni,Qian Lei, Tao Chun-hu, Liu Xin-ling. Damage mode and failure mechanism of cementing structure [J]. Failure Analysis and Prevention, 2012, 7(3): 162–166.
2. Hongze Wang, Motoki Nakanishi, Yosuke Kawahito. Effects of welding speed on absorption rate in partial and full penetration welding of stainless steel with high brightness and high power laser [J].Journal of Materials Processing Technology, 2017, 249: 193–201.

3. Pengfei Bai, Zhijiang Wang, Shengsun Hu, Shangwen Ma, Ying Liang. Sensing of the weld penetration at the beginning of pulsed gas metal arc welding[J]. *Journal of Manufacturing Processes*, 2017, 28(1):343–350.
4. Yi-Chun Liao, Ming-Huei Yu. Effects of laser beam energy and incident angle on the pulse laser welding of stainless steel thin sheet [J]. *Journal of Materials Processing Tech*, 2007, 190(1–3):102–108.
5. MENG Xianghai, LI Mengxing, WU Lixue, LI Yungang. Analysis and countermeasure of defects in welding automobile galvanized steel sheet [J]. Foundry Technology, 2018, 39(3): 625–627.
6. Weichiat Chen, Paul Ackerson, PalMolian. CO2 laser welding of galvanized steel sheets using vent holes[J]. *Materials & Design*, 2009, 30(2): 245–251.
7. Wilfried Reimann, SimonPfriem, Thorge Hammer, Dieter Päthe, Michael Ungers, Klaus Dilger. Influence of different zinc coatings on laser brazing of galvanized steel[J]. *Journal of Materials Processing Tech*, 2017, 239:75–82.
8. Hui Huang, Jiandong Wang, Liqun Li, Ninshu Ma. Prediction of laser welding induced deformation in thin sheets by efficient numerical modeling [J]. *Journal of Materials Processing Technology*, 2016, 227:117–128.
9. Matsuoka S, Okamoto Y, Okada A. Influence of weld bead geometry on thermal deformation in laser micro-welding[J]. *Procedia CIRP*, 2013, 6:492–497.
10. M.Seyyedian Choobi, M.Haghpanahi, M.Sedighi. Prediction of welding-induced angular distortions in thin butt-welded plates using artificial neural networks[J]. *Computational Materials Science*, 2012, 62:152–159.
11. Liu Jia. Research on laser lap welding technology of SUS301L austenitic stainless steel for railway vehicles [D]. Changchun: Changchun University of Science and Technology, 2012.
12. Fang H Y.Welding structure [M].Beijing:China Machine Press, 2008.
13. Tan Zhen, Guo Guangwen. Thermophysical properties of engineering alloys [M].Beijing: Metallurgical industry press, 1994.

Figures

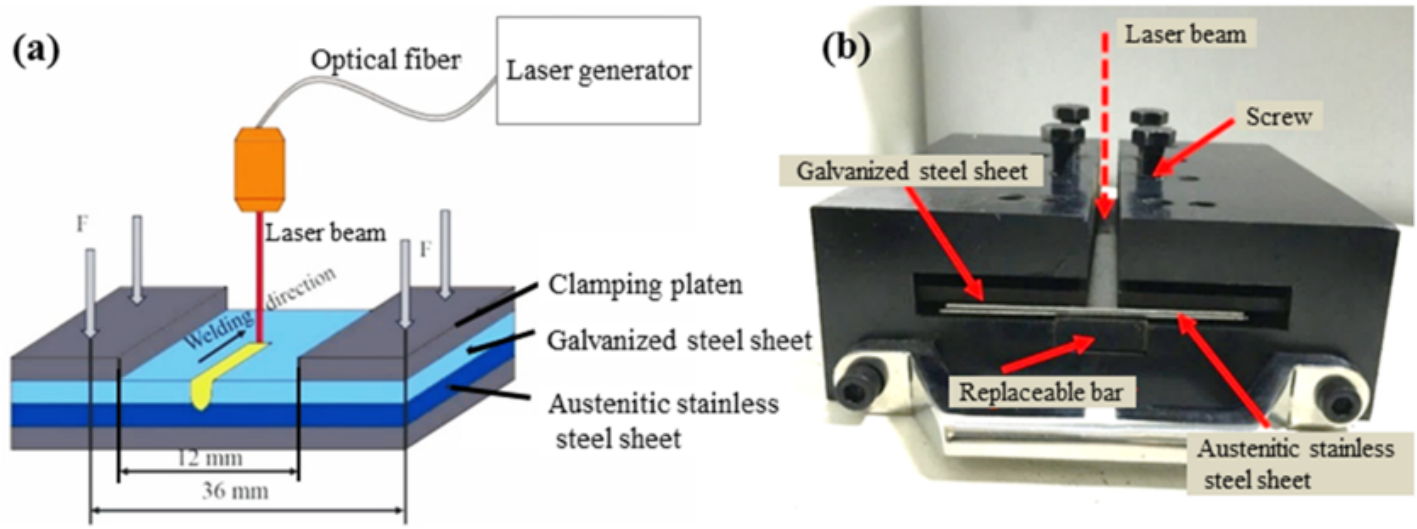

Figure 1

Schematic diagram of non-penetration lap laser welding experiment (a) schematic diagram of non-penetration lap laser welding process; (b) photo of welding fixture.

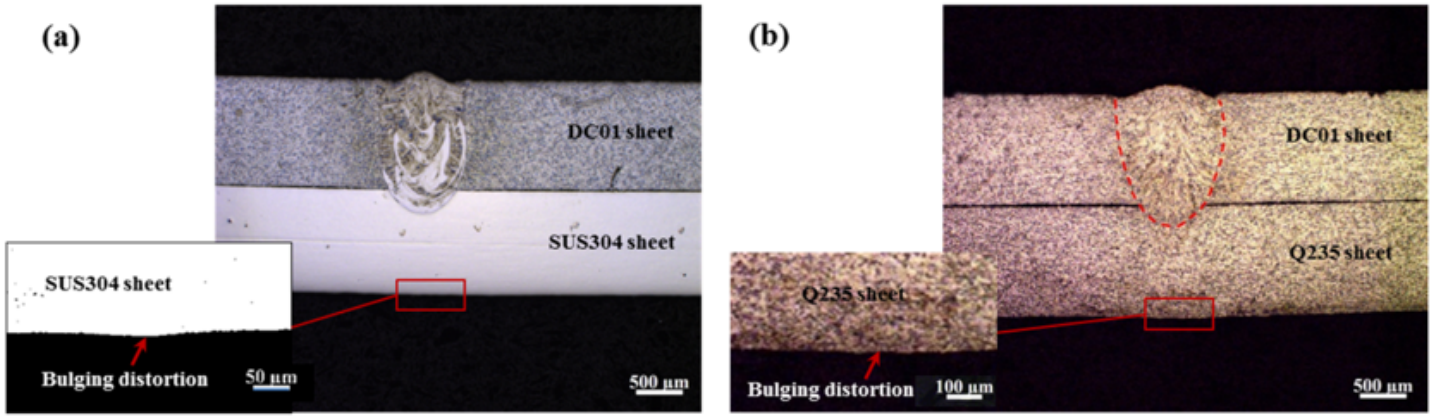

Figure 2

Cross-section of non-penetration lap laser welded joint and the morphology of the bulging distortion on the partially penetrated side of SUS304 and Q235 steel sheets: (a) the lap welded joint of DC01 galvanized steel and SUS304 austenite stainless steel sheets; (b) the lap welded joint of DC01 galvanized steel and Q235 carbon steel sheets.

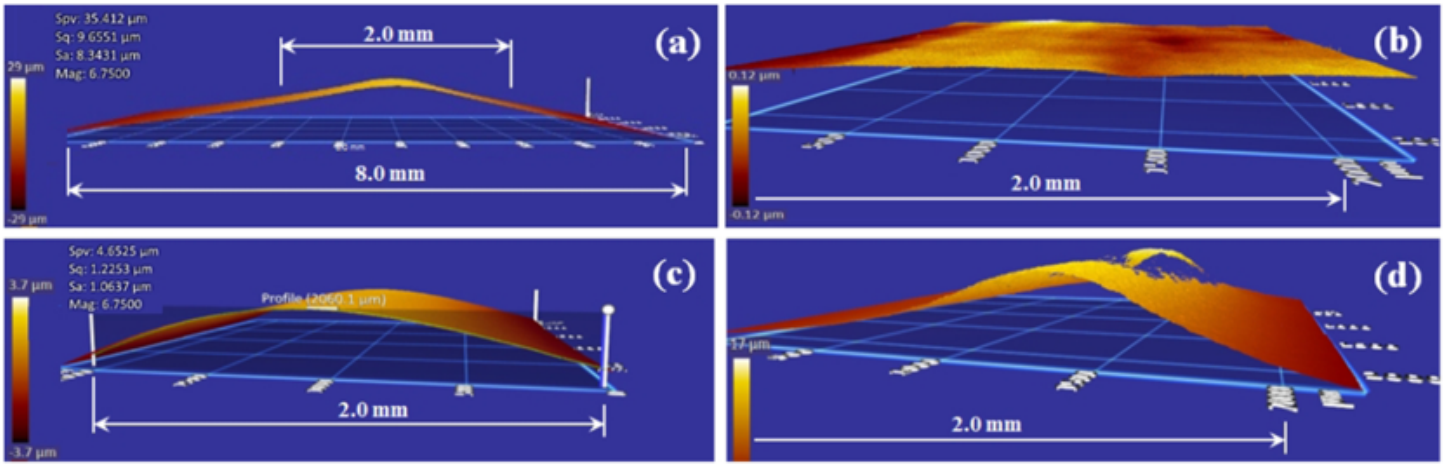

Figure 3

3D contour model of the bulging distortion detected of the SUS304 sheet of the lap welded joint by laser profiler: (a) the welded joint with a laser power of 2.4 kW, in which the scanning width of the profiler is 8 mm; (b) the SUS304 sheet before welding, in which the scanning width of the profiler is 2 mm; (c) the welded joint with a laser power of 2.0 kW, and the scanning width of the profiler is 2 mm; (d) the welded joint with a laser power of 2.6 kW, in which the scanning width of the profiler is 2 mm.

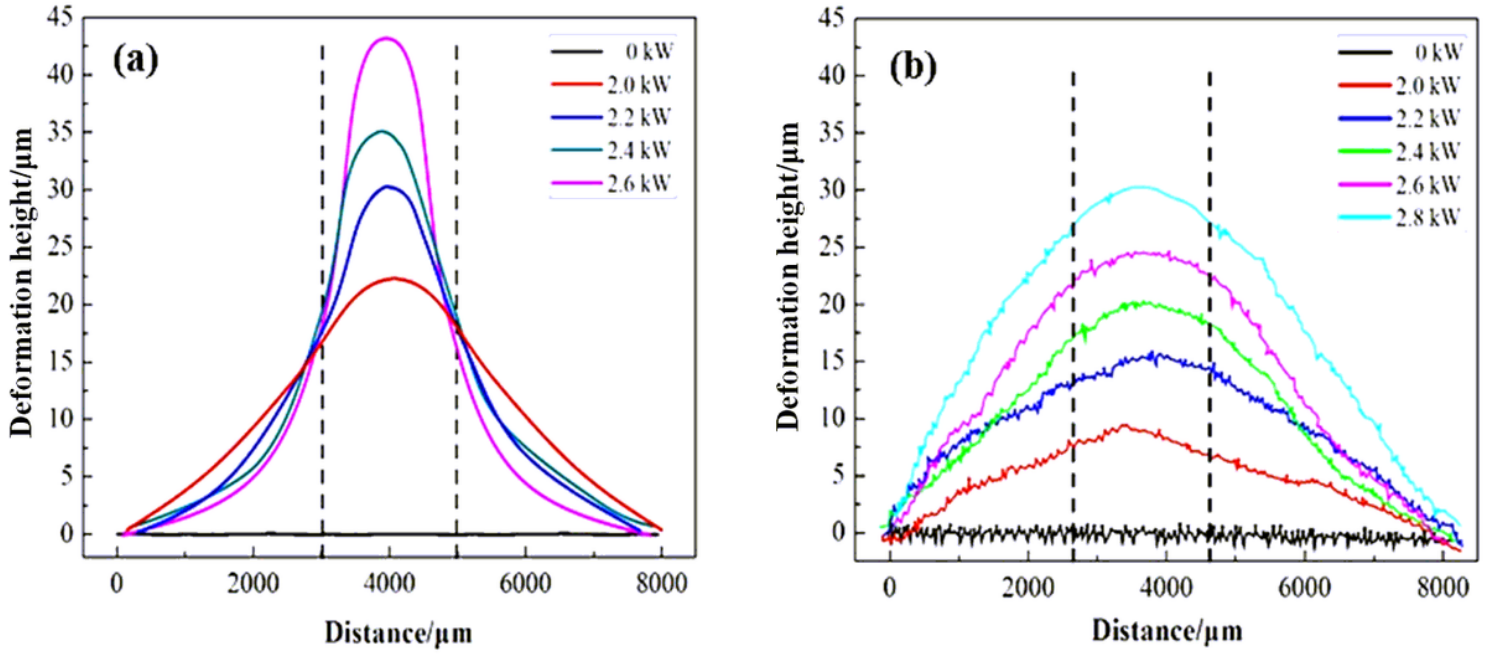

Figure 4

The outline curves of the deformation on the partially penetrated side of the lap laser welded joints at different laser welding power (a) the lap welded joint of DC01-SUS304 steel plates; (b) the lap welded joint of DC01-Q235 steel plates.

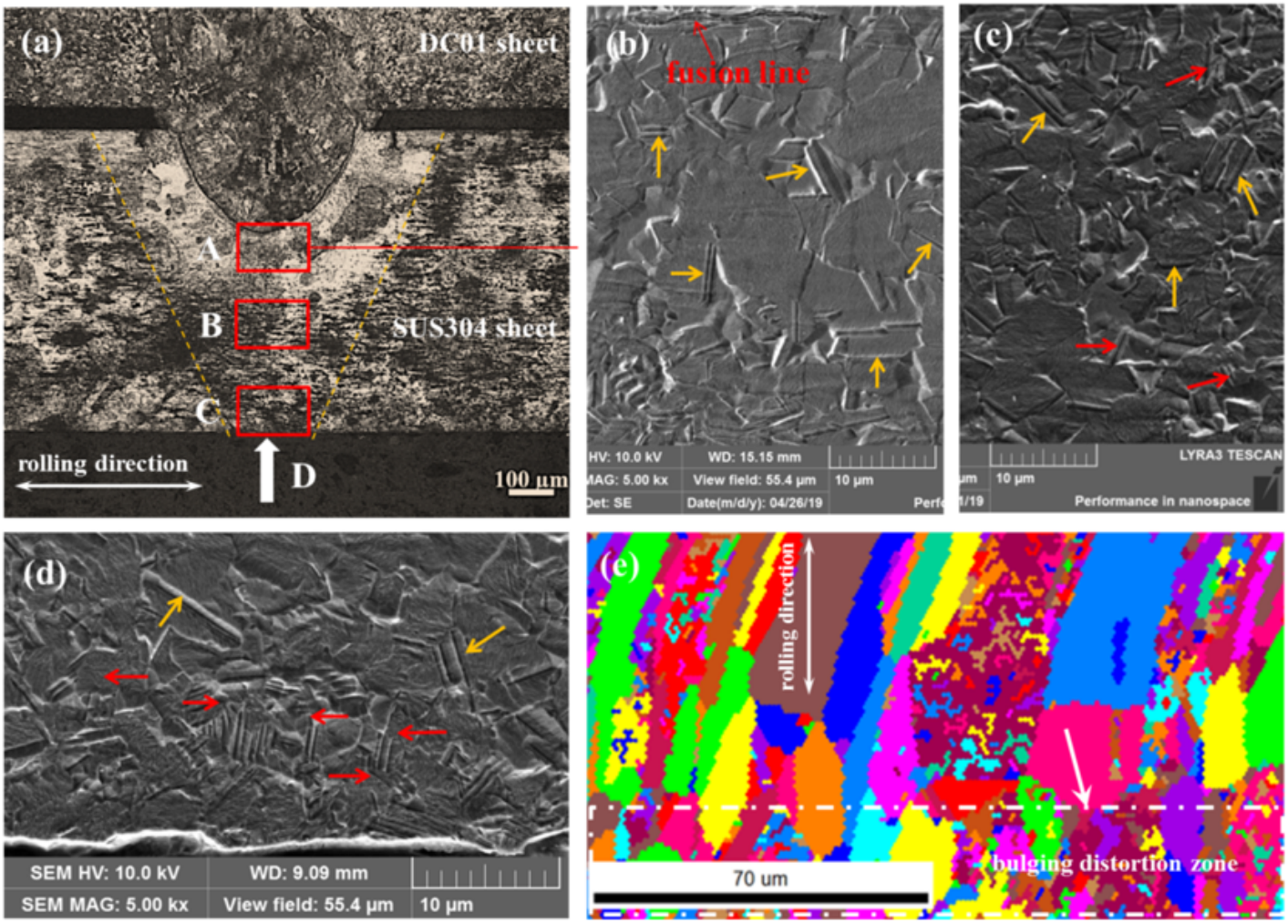

Figure 5

Cross-section morphology of the lap welded joint and microstructure of the SUS304 steel sheet on the partially penetrated side. (a) the lap welded joint (b) SEM microstructure at the “B”mark in (a), where the yellow arrow indicates annealed twins; (c) SEM microstructure at the “B” mark in (a), where the yellow arrow indicates annealed twins; (d) SEM microstructure at the “C” mark in (a), where the red arrow indicates deformation twins; (e) EBSD grain map of the backsurface of the partially penetrated side of the SUS304 sheet, at the “D” mark in (a). In the bulging distortion zone shown by the arrow, the elongated fiber grains in the original state have been recrystallized into equiaxed grains.

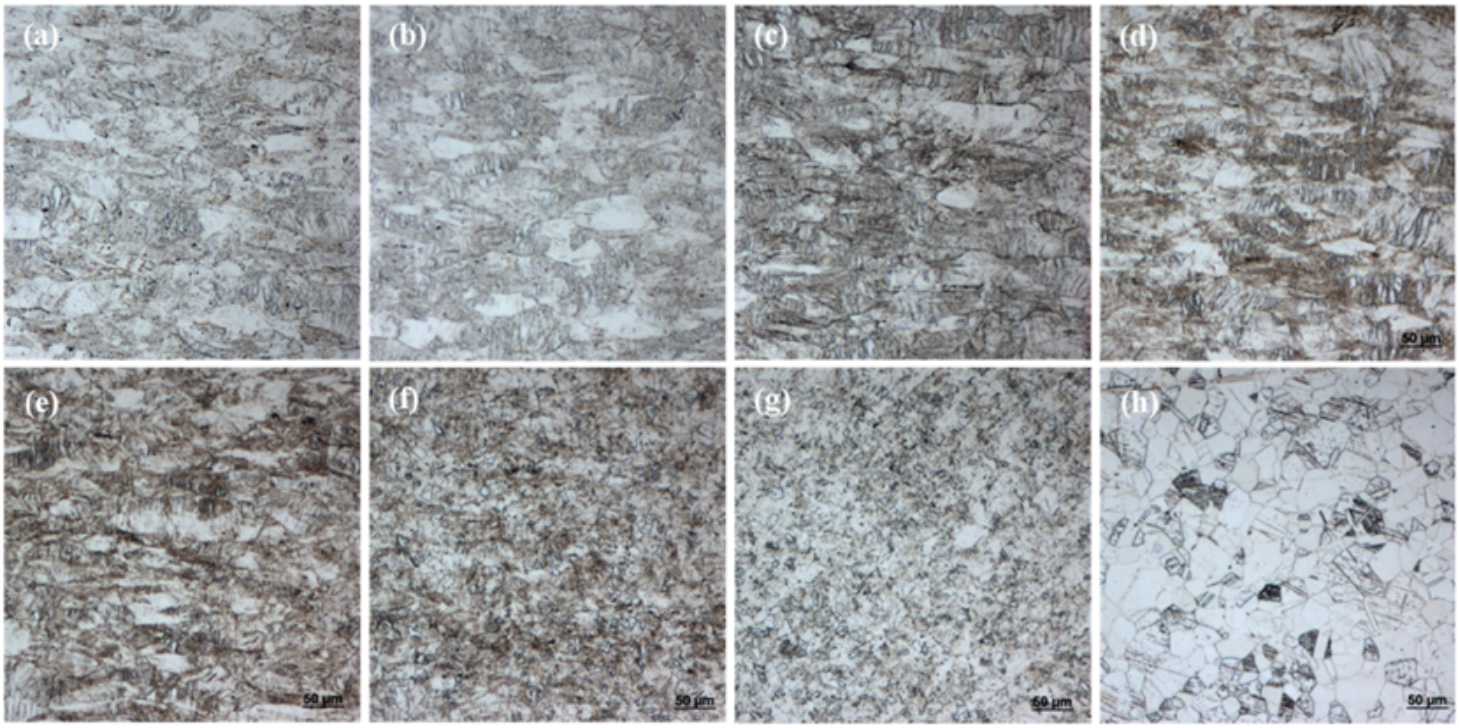

Figure 6

Microstructure of cold-rolled SUS304 stainless steel sheet heated at different temperatures for 5 minutes, and water quenched: (a) 300℃; (b) 400℃; (c) 500℃; (d) 600℃; (e) 700℃; (f) 800℃; (g) 900℃; (h) 1000℃, the original cold rolled grains have been completely recrystallized into equiaxed grains.

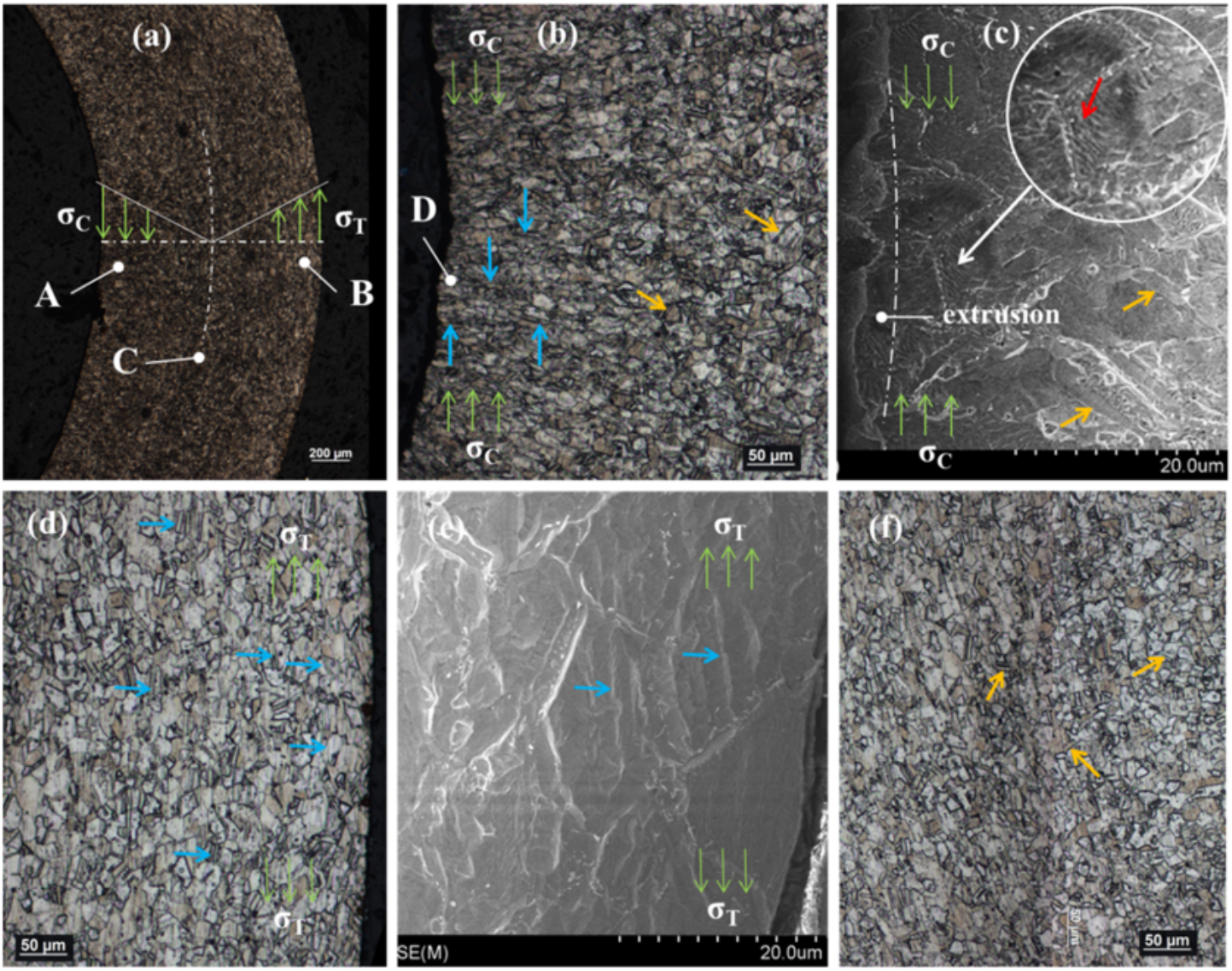

Figure 7

Morphology and microstructure of the cross-section of cold-rolled SUS304 stainless steel sheet after heating at 1000°C for 5 minutes, bending, and water quenching. (a) the cross-section of the bent sheet, where σC-compressive stress, σT-tension stress; (b) at the “A” mark in (a), the optical micrograph of the interior arc of the bent sheet, where the twin planes shown by the blue arrows are perpendicular to the rolling direction; (c) SEM micrograph at “D” mark in (b), where the red arrow shows deformed twins, and the yellow arrows show annealed twins, and the area shown by dotted line is the extrusion deformation zone; (d) at the “B” mark in (a), the optical micrograph of the exterior arc of the bent plate, where the twins planes shown by the light arrows are parallel to the rolling direction; (e) SEM micrograph at the “B” mark in (a), where the twin planes shown by the light blue arrows are parallel to the tensile stress.; (f) at the “C” mark in (a), the optical micrograph of the core of the bent plate, where the annealed twins shown by the yellow arrow have no obvious directionality.

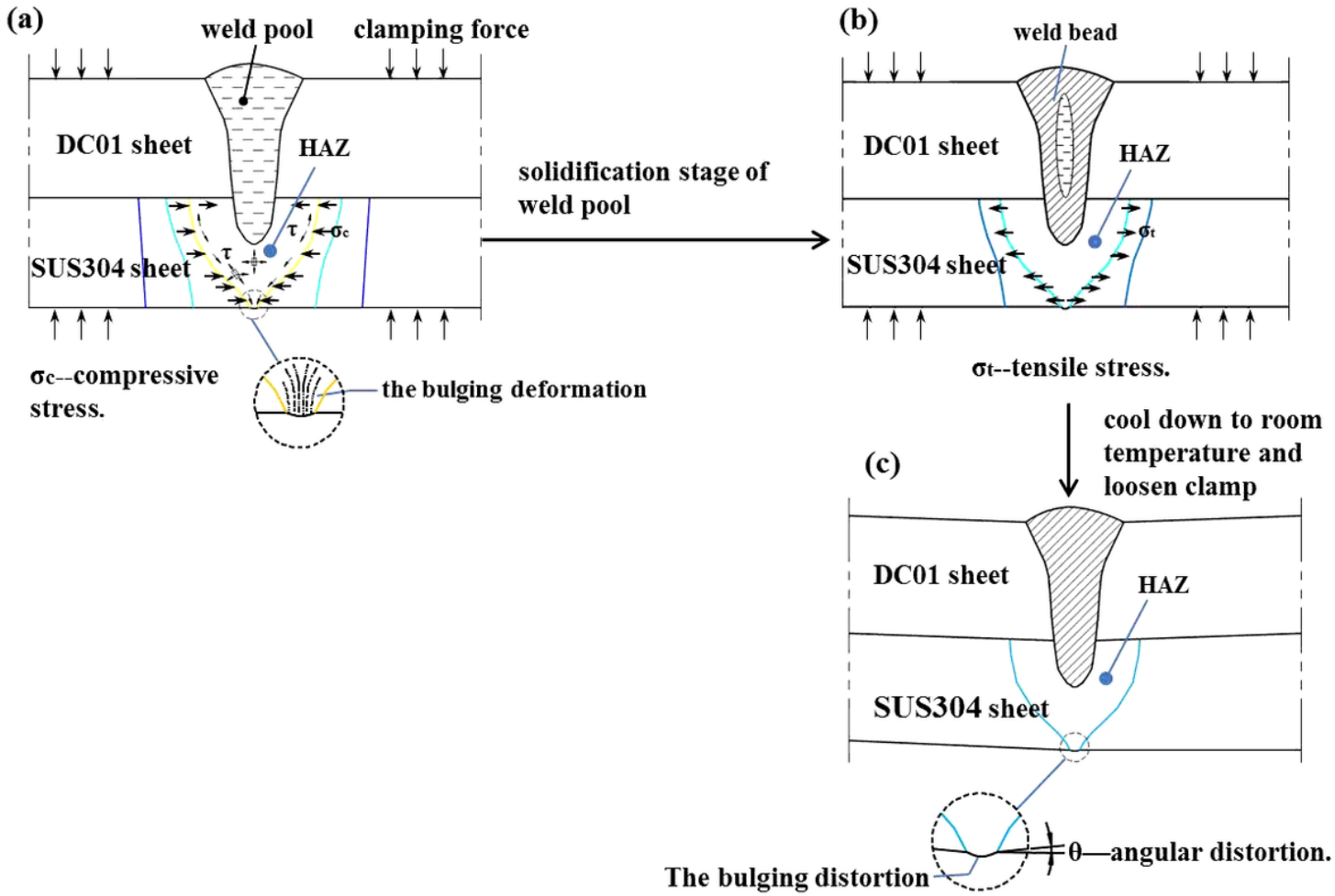

Figure 8

Schematic diagram of the bulging distortion on the partially penetrated side of SUS304 austenitic stainless steel sheet of the non-penetration lap laser welded joint: (a) formation stage of weld pool: the compressive stress is generated in the heat-affected zone, and causes the bulging deformation on the partially penetrated side; (b) solidification stage of weld pool: the compressive stress in the heat-affected zone transforms into tensile stress; (c) cool down to room temperature and loosen clamp: the lap welded joint shows angular deformation on the macroscopic scale, while the bulging deformation on the microscopic scale is still retained.